IX International Conference on Computational Methods in Marine Engineering
MARINE 2021
I.M. Viola and F. Brennan (Eds)

# ANALYSIS OF BIOMIMETIC STREAM ENERGY DEVICE BASED ON FLAPPING FOILS

**IRO MALEFAKI[1], DIMITRA ANEVLAVI[2] AND KOSTAS BELIBASSAKIS***
School of Naval Architecture & Marine Engineering
National Technical University of Athens, Greece
NTUA Campus, 15780 Athens, Greece
[1]https://sites.google.com/view/iromalefaki/
[2]https://sites.google.com/view/dimitraanevlavi
*e-mail: kbel@fluid.mech.ntua.gr - web page: http://arion.naval.ntua.gr/~kbel/

**Key words:** Biomimetic systems, stream energy converter, flapping foil, vortex-induced vibration stream energy converter

**Abstract.** In this work, the performance of biomimetic device that consists of including a rotating, vertically mounted, biomimetic wing, supported by an arm linked at a pivot point on the mid-chord is evaluated using a numerical model is considered and results are presented concerning the performance. Activated by a controllable self-pitching motion, the system performs angular oscillations around the vertical axis in incoming flow. The performance of the above flapping-foil, biomimetic flow energy harvester, is calculated and the results are compared against experimental data. By systematical application of the model the power extraction and efficiency of the system is presented for various cases including different geometric, mechanical, and kinematic parameters, and the optimal performance of the system is determined. Also comparisons of the calculated performance are presented against predictions for other tidal energy devices, such as the stream energy converters based on the vortex-induced angular oscillations of a cylinder.

## 1 INTRODUCTION

Biomimetic stream energy harvesting devices based on oscillatory hydrofoils have been considered for operation in the marine environment; see [1,2,3]. Unlike conventional turbines, the above energy converters operate at relatively low tip speed, are more environmentally friendly in terms of noise generation, thus reducing impact on the communication and navigation of aquatic animals. One type represents systems that demand controlling/actuating the pitching motion, namely the semi – activated oscillating hydrofoils. Existing applications of the flapping type energy harvesters in industry are often based on this design, where energy input is needed to activate the pitching motion, whereas energy harvesting is achieved through the resulting heaving motion generated by fluid dynamic lifting forces. Positive net energy extraction is possible only in cases where the energy extracted from the heaving motion is greater than the energy expenditure to activate the pitching motion. Another advantage of semi-activated biomimetic stream energy converters is that they perform oscillations with

respect to more than one degree of freedom, and one oscillatory motion is controllable. This supports optimized operation as compared to conventional hydro-turbines, which are characterized by a single degree of freedom and their performance is strongly dependent on the ratio of the blade-tip speed to incident-flow speed and the uniformity of the incoming flow.

Several design configurations for semi – activated hydrofoils have been proposed as biomimetic stream energy devices [1], with variations in the way which the foil motion is constrained. In the same direction of research, Huxham et al. [4] conducted a laboratory experiment in a water tunnel in the University of Sydney. The device consists of a vertically aligned aluminum NACA0012 foil with span equal to s=0.34 m and chord c=0.1 m, pivoted at a point located at $1/4^{th}$ of its chord from the leading edge, and linked to a vertical axis by an arm of 0.3m length. Additionally, the edges of the foil are placed near the ceiling and the floor of the water tunnel in order to reduce the 3D effects and the induced drag. The heave of the foil is not prescribed, but is dependent on the response of the system due to hydrodynamic forcing on the foil. The purpose of the study was to determine the influence of the pitch amplitude and reduced frequency on the power generation as well as the overall efficiency of the system. Many tests were conducted in order to determine the effects of these parameters with flow speed of $U = 0.5$ m/s and given power-take-off characteristics. The above concept has been further exploited by the BioSTREAM device developed by BioPower Systems Pty Ltd; see [5]. The aforementioned device is based on the principle of oscillating hydrofoils for tidal stream power generation. The foil is attached to an arm, and is therefore restricted to a circular motion. The components of the forces acting on the hydrofoil tangentially to the arm, serve to either accelerate or decelerate the foil, while the hydrofoil resembles a fish tail. A prototype device is to be built and installed in a tidal stream off Flinders Island; see Fig. 4 in Ref. [5].

Apart from the oscillating hydrofoils, another concept that exploits flow-induced oscillatory motions of bluff bodies for energy harvesting has received considerable attention in recent years. Various aspects and pertinent phenomena have been investigated with a view to assess the performance and optimize the design of hydrokinetic energy converters in several studies. Vortex-induced vibration (VIV) is a known phenomenon , mostly unwanted as it compromises the integrity of equipment, such as heat-exchanger tubes, oil risers, offshore platforms, transmission cables, cable-stayed bridges, tall chimneys, etc. due to fatigue of the structural components. However, it may be purposefully enhanced in hydrokinetic energy converters where electricity can be produced e.g. by electromagnetic induction through the oscillating components. These converters are based on the idea of maximizing rather than spoiling vortex shedding and exploiting rather than suppressing VIV. This phenomenon occurs over very broad ranges of Reynolds (Re) number. As a result, even from currents as slow as 0.25 m/s, such devices are able to extract energy with high power conversion ratio, making ocean/river current energy a more accessible and economically viable resource. The best-known concept is the VIVACE converter developed by the Marine Renewable Energy Laboratory (MRELab) in the University of Michigan [6,7].

In this work, a semi-3D model based on unsteady hydrofoil theory [8] is applied to the performance of the above flapping-foil, biomimetic stream flow energy harvester. Results obtained with the proposed numerical model concerning the performance of the biomimetic device including a rotating, vertically mounted, biomimetic wing, supported by an arm linked at a pivot point on the mid-chord are presented; see [8]. Activated by a controllable self-

pitching motion the system performs angular oscillations around the vertical axis in incoming flow. The performance of the above flapping-foil biomimetic flow energy harvester is calculated and the results are compared against experimental data [4]. Also, comparisons of the calculated performance are presented against predictions for a stream energy device, based on vortex-induced angular oscillations of a cylinder which is studied in more detail in Ref. [9].

## 2 MODEL OF BIOMIMETIC STREAM ENERGY CONVERTER

We assume a semi-activated water stream energy converter, that consists of a foil performing an angular oscillatory motion around the vertical axis $Oz$ due to an enforced prespecified self-pitching angular oscillatory motion around the pivot axis PP'; see Fig.1. The hydrofoil is connected with an arm of length $R$ from $Oz$ to the pivot point, and has two degrees of freedom as defined by the angular motions $\theta$ and $\phi$. For small angles $\phi$ the combined motion corresponds to enforced pitch $\theta$ and an induced heave-like motion Rφ in the transverse $y$-direction, with phase difference around 90deg, resembling the motion of a flapping wing. The foil is symmetric and the pitch motion is prescribed, while the heave motion is induced by the interaction of the surrounding flow field with the foil essentially due to the effect of instantaneous angle of attach $\alpha$. The supporting system is modeled as a spring, and the power-take-off system modeled as a damper.

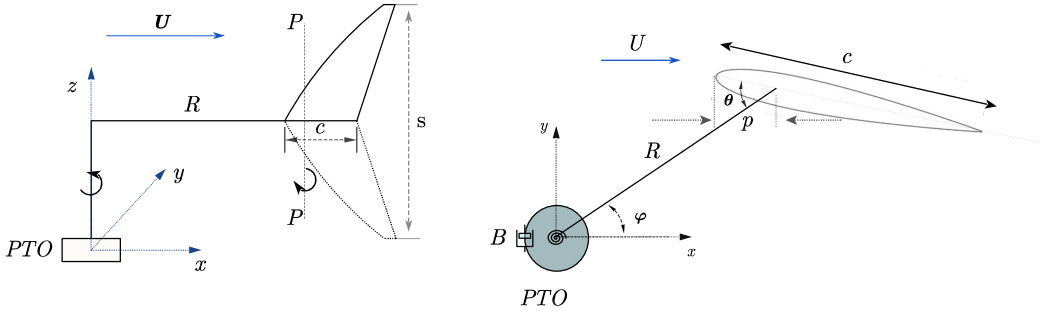


**Figure 1:** The studied biomimetic flow energy harvester (left), and cross-section of the biomimetic flapping foil operating in uniform inflow with velocity $U$ (right).

The model used in this study is based on the thin foil approximation by Theodorsen, extended to include added-mass forces as well as the effect of shed vorticity, see eg. Katz & Plotkin [10]. Using linear analysis, the present model provides an analytical expression of the hydrodynamic forces and moments on a zero-thickness foil undergoing harmonic oscillation in a uniform stream. Owing to its simplicity, it has been widely employed in the investigation of unsteady foil dynamics and flow-induced instability.

Assuming that the fluid surrounding the foil and the wake is inviscid, incompressible and irrotational and that each section of small thickness wing undergoes small-amplitude pitching and heaving harmonic oscillations, the sectional lift coefficient is given by:

$$C_L = \frac{F_L}{0.5\rho U^2 c} = 2\pi U^{-1} C(k)\left[U\theta - \dot{h} + \left(\frac{3}{4} - \frac{p}{c}\right)c\dot{\theta}\right] + \frac{\pi c}{2U^2}\left[\left(U\dot{\theta} - \ddot{h}\right) + c\left(\frac{1}{2} - \frac{p}{c}\right)\ddot{\theta}\right], \quad (1)$$

where an over-dot denotes time-differentiation, $k=\frac{\omega c}{2U}$ is the reduced frequency, and $C(k)$ denotes the Theodorsen function, which under the assumption of harmonic oscillatory motion with an $\exp(i\omega t)$ time dependence, is expressed as a ratio of the Hankel functions of the second kind as follows (see Katz & Plotkin [10]):

$$C(k)=\frac{H_1^{(2)}(k)}{H_1^{(2)}(k)+iH_0^{(2)}(k)}. \tag{2}$$

Moreover, the moment per unit span required to pitch the foil with respect to the pitching axis, is approximated by the following equation (see [10], Sec.13.8):

$$\begin{aligned} C_M=\frac{M}{0.5\rho U^2 Ac}=-\frac{\pi c}{2U^2 A}\Bigg\{ & c\left(\frac{p}{c}-\frac{1}{2}\right)\ddot{h}+Uc\left(\frac{3}{4}-\frac{p}{c}\right)\dot{\theta}+\frac{c^2}{4}\left(\frac{9}{8}+\frac{4p^2}{c^2}-\frac{4p}{c}\right)\ddot{\theta}+ \\ & -\left(\frac{4p}{c}-1\right)UC(k)\left[-\dot{h}+U\theta+c\left(\frac{3}{4}-\frac{p}{c}\right)\dot{\theta}\right] \end{aligned} \tag{3}$$

The 3D coefficients are obtained by a strip-wise integration along the span of the wing

$$C_{L,3D}=\frac{F_{L,3D}}{0.5\rho U^2 A}=\frac{C_{3D}}{0.5\rho U^2 A}\int_{span}F_L ds,\; C_{M,3D}=\frac{M_{3D}}{0.5\rho U^2 Ac_m}=\frac{C_{3D}}{0.5\rho U^2 Ac_m}\int_{span}M ds \quad , \tag{4}$$

where $A$ is the wing planform area and $c_m$ the midchord length. In addition, $C_{3D}$ is a correction factor taking into account 3D-effects due to the free vorticity. This effect is approximated from steady lifting line theory for elliptical wings as $C_{3D}=AR/AR+2$, with $AR=s^2/A$ denoting the aspect ratio of the wing. Obviously, for a flapping wing with an orthogonal planform shape, with constant spanwise chord length distribution, it holds $C_{L,3D}=C_{3D}C_L, C_{M,3D}=C_{3D}C_M$.

### 2.1 Calculation of the performance of the biomimetic stream energy converter

The hydrofoil is connected through the arm *R* to the vertical axis, the power-take-off system is modelled with a rotational spring of constant *C* and a damper with coefficient *B*; see Fig. 1 (b). The dynamics governing the oscillatory motion of the considered device are obtained from the balance of angular momentum about the vertical axis $OX$,

$$I\ddot{\phi}(t)+B\dot{\phi}(t)+C\phi(t)=T(t) \quad , \tag{5}$$

where $\phi(t)$ represents the angular response of the system (see Fig.1), $I$ is the moment of inertia of the foil including the connecting arm, $B$ is the damping coefficient which represents the energy extraction from the generator (power-take-off), $C$ is the rotational spring constant, and $T$ represents the generated torque. The power extraction is achieved by the generated torque which is essentially provided by the lift force of the dynamic foil and is affected by the corresponding drag force. Thus, maximizing the torque can increase the

amount of the output power. We next consider the self-pitching oscillation of the foil defined as a simple periodic function of time of angular frequency ω and amplitude $\theta_0$:

$$\theta(t) = g(t)\theta_0 \cos(\omega t) \quad , \tag{6}$$

where $g(t)$ is a filter function enabling the smooth enforcing of the self-pitching motion, the generation of lifting flow with angle of attack and the angular response of the system. Moreover, the derived transverse heaving motion of the foil is:

$$h(t) = R\phi(t)\cos\left(\phi(t)\right) \, , \tag{7}$$

which in the steady-state condition and small responses $|\phi| \ll 1$ results in harmonic oscillations with amplitude $\phi_0$ and induced transverse (heaving) motion of amplitude $h_0 \approx R\phi_0$.

As the foil oscillates in the uniform current, the relative flow velocity due to the rotational motion of the wing about the vertical axis $Ox$, in conjunction with the incident parallel flow, is $\mathbf{U}_{rel} = \mathbf{U} - \mathbf{U}_{fin}$, where $\boldsymbol{U}_{fin}$ is the corresponding rotational velocity of the wing $\mathbf{U}_{fin} = \dot{h}\mathbf{e}_\phi = R\dot{\phi}\mathbf{e}_\phi$, acting in the tangential direction with $\mathbf{e}_\phi$ denoting the corresponding unit vector. On the other hand, the self-pitching motion of the foil is taken into account for the formation of the angle of attack, and results in the change of the effective angle of attack of the flow relative to the foil is given by

$$\alpha(t) = \theta(t) - \gamma(t) \, , \tag{8}$$

where the latter component describes the effect of the induced transverse heaving motion due to the rotational along the vertical axis oscillatory motion of the wing

$$\gamma(t) = \tan^{-1}\left(\frac{U_{fin}}{U}\right) = \tan^{-1}\left(\frac{\dot{h}}{U}\right) \, . \tag{9}$$

Based on the above the most important parameters concerning the response and the performance of the examined system are: (i) the amplitude of the enforced self-pitching motion $\theta_0$ (ii) the location of the foil pivot axis with respect to the foil leading edge $p/c$ (iii) the dimensionless heave amplitude $h_0/c$. In addition, the most important flow dimensionless parameters, which define the dynamic behavior of the system are: (i) the reduced frequency $k = \frac{\omega c}{2U}$ and the Strouhal number $St = \frac{\omega h_0}{\pi U} \approx \frac{\omega R\phi_0}{\pi U}$ (ii) the amplitude of the effective angle of attack $\alpha_0$, (iii) the Reynolds number $\mathrm{Re} = \frac{Uc}{\nu}$ through which, in conjunction with the instantaneous angle of attack, the drag forces are estimated. To proceed further we assume that the response of the system activated by the self-pitching motion (defined by Eq.6) is a function of time and thus the generated torque is equal to

$$T(t) = RF_\theta(t) \, , \tag{10}$$

where $F_\theta$ is the projection of the hydrodynamic forces in the tangential direction

$$F_\theta(t) = F_{L_\theta}(t) - F_{D_\theta}(t). \tag{11}$$

In order to take into account leading-edge suction force effects in this work, the instantaneous lift force is assumed to act on the hydrofoil in the transverse y-direction, and is given by (see also Fig. 3 in Ref. [8]):

$$F_{L_\theta}(t) = F_L(t)\cos\left(\varphi(t)\right), \tag{12}$$

The lift force $F_L$ is estimated through the lift coefficient by means of Eqs.(1) and (4), and the drag force is obtained by a drag coefficient calculated by means of the following empirical formula,

$$F_D = C_f(\mathrm{Re}) + C_a\alpha^2(t), \tag{13}$$

where the first term $C_f(\mathrm{Re})$, with Re denoting the characteristic Reynolds number, represents skin friction effects, and the second term models the effect of the dynamic angle of attack $\alpha(t)$ expressed through the empirical coefficient $C_\alpha$; see also Filippas & Belibassakis [11]. Substituting the above equations into the equation of motion, Eq. (5), in the simple case of a wing with orthogonal planform (constant chord distribution along the span, as in the case studied experimentally in Ref.[4]) we obtain the following dynamic equation modelling the angular response and the performance of the examined system:

$$\begin{aligned} I\ddot{\varphi}(t) + B\dot{\varphi}(t) + C\varphi(t) = {} & R\cos\varphi(t)\left\{\left(\frac{1}{2}\pi\rho UAC_{3D}C(k)\left[U\theta - \dot{h} + \left(\frac{3}{4} - \frac{p}{c}\right)c\dot{\theta}\right]\right)\right\} + \\ & + R\cos\varphi(t)\left\{\frac{\pi\rho cAC_{3D}}{4}\left[\left(U\dot{\theta} - \ddot{h}\right) + c\left(\frac{1}{2} - \frac{p}{c}\right)\ddot{\theta}\right]\right\} - 0.5R\rho U^2 A\sin\varphi(t)\left\{\left(C_f + C_a\alpha^2\right)\right\} \end{aligned} \tag{14}$$

Since the power-take-off system is idealized as a simple damper, the instantaneous power output is calculated by:

$$P_{output}(t) = B\dot{\varphi}^2, \tag{15}$$

and the time average power output can be calculated using the results of the system, which in the case of harmonic response at angular frequency ω is: $P_{output} = 0.5B\omega^2\left|\phi_0\right|^2$. The external moment $M$ required to drive the enforced pitching motion equals to the hydrodynamic moment, Eqs.(3) and (4), and thus, we can calculate the power input required to rotate the hydrofoil. The average power spent in order to pitch the foil is expressed by:

$$P_{input} = -\int_0^T M_{3D}(t)\dot{\theta}(t)\,dt\ . \tag{16}$$

The energy extraction efficiency $\eta$ is chosen in the present study to be defined as the ratio between the cycle-averaged power extracted and the energy flux of the incoming flow, as follows:

$$\eta = \left(P_{output} - P_{input}\right)/\left(0.5\rho U^3 sd\right)\ , \tag{17}$$

where $d$ denotes the distance between the extreme points in the transverse direction during the oscillatory motion of the system, and the quantity in the denominator is the incoming power flux of the uniform incident flow through the section swept by the oscillating foil.

**2.2 Numerical results**

In order to validate the accuracy of the method, the results obtained with the present method are initially compared against the experimental data provided by Huxham et al. [4]. For this purpose, a rectangular wing NACA0012 sections is modelled. Following the experimental set-up, the foil has constant chord distribution $c = 0.1m$ along the span that is equal to $s = 0.34m$. In this particular arrangement the pivot point is located at position $p/c = 1/4$ of its chord, and it is connected to the vertical axis using an arm of $R = 0.3m$ length. The aspect ratio of the foil is therefore $AR = 3.4m$. However, the foil edges located very close to the water tunnel ceiling and floor peform like end-plates in order to minimize the tip vortices. This results in the reduction of the induced drag and the 3D effects on the flow, and consequently the efficiency of the configuration and the performance of device are increased. The lift and drag of the foil create a moment at the axis of rotation of the arm and a sensor is placed at the shaft to measure this moment (see Fig.2 in Ref. [4]). Two identical torque transducers are used to measure the torque needed for the self-pitching motion of the foil. A dashpot is placed on the arm shaft to dampen the motion modelling also the power-take-off generator.

In order for the present method to better simulate the experiment, an artificial increased value of the aspect ratio $AR = 10$ is considered, so that the effect of the nearby boundaries in the vicinity of wingtips on the reduction of the tip wake vortices are taken into account, with the corresponding results as compared with the measured data provided by [7].

In Fig. 2, the response of the system is illustrated, as calculated by the present method. Results are obtained by considering no spring constant ($C = 0$) and a dimensionless damping coefficient $B' = B/\left(\tfrac{1}{2}\rho U s c^2 R\right) = 29.5$, as reported in [4]. More specifically, the time history of the angle of attack and the enforced self-pitching angle are shown for onset flow speed $U = 0.5\,m/s$ and reduced frequency $k = 0.1$. It is further observed that the amplitude of the response is calculated to be $\phi_0 = 7.85^\circ$, and the corresponding amplitude of the effective angle of attack is found to be $\alpha_0 = 37.54^\circ$. The predictions by the present model are very close to the experimental data which are reported to be: $\phi_0 = 7.85^\circ, \alpha_0 = 38.2^\circ$, respectively It is clearly observed that the present method results are in good agreement with the experimentally measured data (available from [4]) when the system has reached its steady-state (periodic) response, although an underestimation of the input power is observed. This is due to the drag force is calculated by the present empirical formula, which does not treat dynamic stall and flow separtion effects. For the considered configuration and case, the power required to drive the self-pitching mechanism of the foil as well as the output power are reported to be 0.51W and 1.42 W, respectively. Thus, the calculated efficiency is 26.1%, which is increased by a relatively small amount as compared to the experimental value which is reported to be 23% in Ref. [4]. Still however, the present simplified method is shown to represent quite well the dynamic response and performance of the considered system.

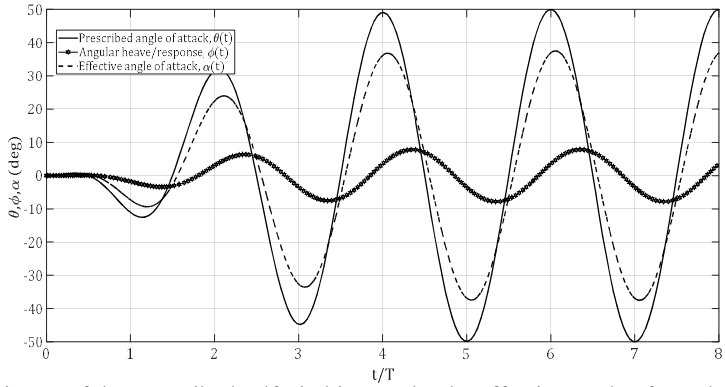


**Figure 2.** Time history of the prescribed self-pitching angle, the effective angle of attack and the angular response of the system as calculated by the present method, for the experimental configuration studied by Huxham et al.[4], for $U = 0.5m/s$, reduced frequency $k = 0.1$, pitching amplitude $\theta_0 = 50\deg$ and dimensionless damping coefficient $C' = 29.5$.

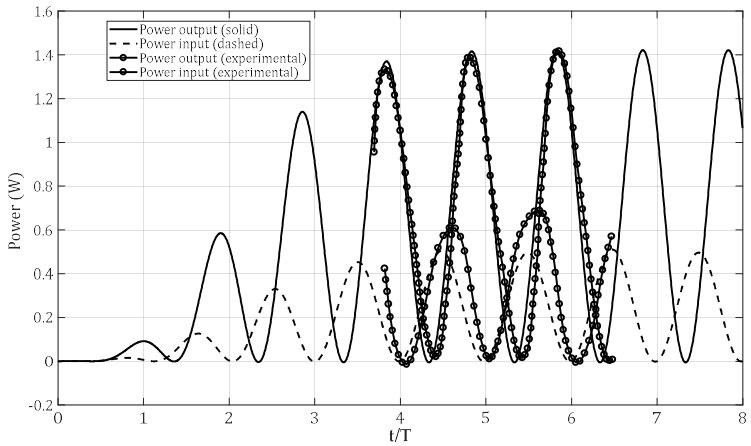


**Figure 3.** Time history of power output and power input calculated by the present method, for the the same case as in Fig.2 and comparison with the experimental data provided by Huxham et al [4], shown by using symbols.

## 3 PERFORMANCE CHARACTERISTICS OF THE BIOMIMETIC DEVICE

The previous study case indicates that the present simplified method is able to represent relatively well the dynamic response and performance of the considered system, and, by taking advantage of its analytical structure, it is very conveniently applied to study the effects of various parameters on the performance of the device. It has been also shown that for low and moderate values of the reduced frequency up to $k = 0.16$, with optimal value around $k = 0.1$, the present dynamical system provides consistent predictions, and for low-amplitude responses the non-linear effects are of secondary importance; see [8] for more details. Thus, a linearized version of the model is developed in the frequency domain and systematically applied to further investigate the effects of various parameters concerning the performance optimization of the studied system.

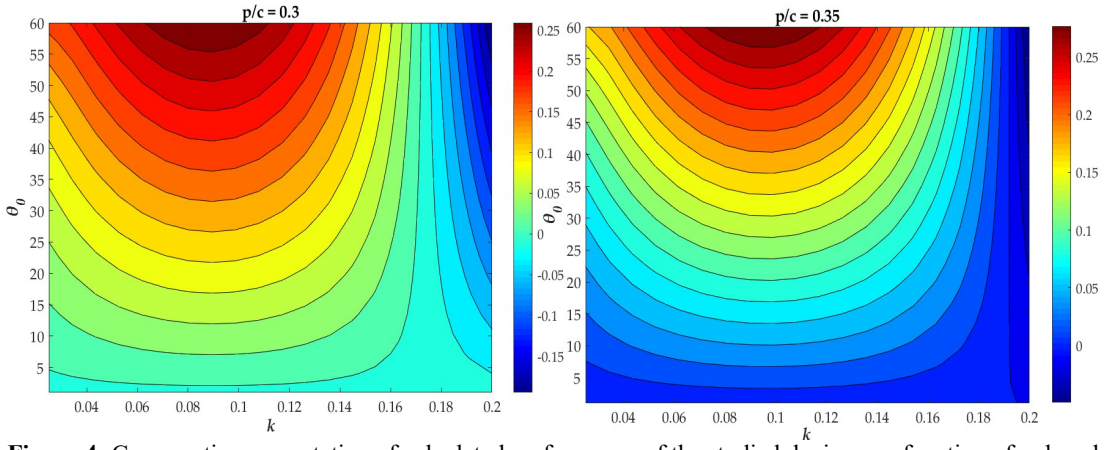


**Figure 4:** Comparative presentation of calculated performance of the studied device as a function of reduced frequency $k = 0.025 \div 0.2$ and pitching amplitude $\theta_0 = 0 \div 60\,\text{deg}$ when the pivot axis is located (a) at $p/c = 0.3$ (left) and (b) $p/c = 0.35$ (right).

For higher values of reduced frequency significant non-linear phenomena take place limiting the predictive capability of the present model, requiring the application of enhanced methods including modelling of dynamic stall effects. However, in the sub-region of parameters where efficient performance of the device occurs the present model still provides good predictions and can be exploited for the optimum selection of parameters concerning the design and the operation of the system.

Following the remarks above, demonstrative results from the parametric study of the device are indicatively presented in Fig.4, where the effect of various important parameters on the performance of the device is highlighted. More specifically, the effect of the location of the pivot axis for the self-pitching motion of the foil on the performance is presented for the same value of the inflow current speed $U = 0.5m/s$, and the damping coefficient modelling the PTO, $C' = 29.5$. In Fig. 4, a contour map of efficiency is plotted as function of the reduced frequency $k$ and the pitching amplitude $\theta_0$ for two locations of pivot axis along the chord of the foil, at $p/c = 0.3$ and $p/c = 0.35$. It is observed in Fig.4 that good efficiency is achieved for a range of reduced frequencies in the Interval $k = 0.06 - 0.11$, and the maximum performance is calculated 26.5% for *k* around 0.1. Moreover, the positioning of the pivot axis is preferably set at a distance around 35% of the chord from the leading edge. The small increase of performance for the latter value of the pivot axis is attributed to the small reduction of input power required due to the corresponding reduced moment for $p/c = 0.3 - 0.35$, which is probably closer at the center of hydrodynamic pressure of the foil in this case for the system in operation conditions around the optimum values.

## 4 VORTEX-INDUCED ANGULAR OSCILLATIONS OF A CYLINDER

In this subsection, indicative results are presented facilitating a first comparative evaluation between two different devices that are based on relatively similar configuration, the semi – activated biomimetic energy converter analyzed in the previous sections of the present work and a hydrokinetic energy converter based on vortex-induced angular

oscillations of a cylinder, which is studied in Ref. [9]. The hydrokinetic energy converter is essentially a modification of the original configuration of the VIVACE [6 ,7] converter. In the design depicted in Fig.5 the cylinder is attached to a supporting arm so that it undergoes vortex-induced angular oscillations with respect to a pivot point. In this configuration, the length of the cylinder-supporting arm offers an additional design parameter to control the system's response and, thereby, the efficiency of hydrokinetic energy conversion. This device has been shown to have potential benefits. However, its performance depends on several design parameters, including the dimensions of the oscillating cylinder and its mass moment of inertia, arm length, damping, stiffness, and current speed. Details concerning the equations describing the kinematics of the problem, which are used to formulate the hydro-dynamical model based on the relative velocity between the cylinder and the free stream, could be found in Ref.[9]. Fig. 5 presents the two-dimensional geometrical model of the problem under consideration as well as the vector diagram of the hydrodynamic forces acting on the cylinder. In this configuration, the pivot point is located downstream of the cylinder. The supporting arm has length $r$ and the main cylinder has diameter $D$. At any instant, the supporting arm forms an angle $\theta$ with respect to the free stream of speed $U$ while the main cylinder moves with linear velocity $U_c$, plotted in the sketch with direction towards the top. The angle is considered positive in the clockwise direction. The linear velocity of the cylinder is $U_c = r\dot{\theta}$, where $\dot{\theta}$ is the angular velocity.

Detailed results concerning the responses and performance of the system are presented in Refs .[8,9]. Selected results from the performed simulations by the non-linear model are presented here in order to proceed to a comparative discussion. In particular, we consider variations of the dimensionless arm length $L^*$, mass ratio $m^*$, damping ratio $\zeta$, and reduced velocity $U^*$. The cylinder response is characterized by the amplitude of angular deflection, denoted $\theta_0$, and the amplitude of displacement transversely to the free stream, $A^* = L\theta_0$. It is noted that $\theta_0$ is dimensionless, since the equation of motion has been solved for the dimensionless angular displacement $\theta^*$, which corresponds to angles normalized with 1 radian. The response $A^*$ and the efficiency $\eta$ of hydrokinetic energy conversion is plotted in Fig.6, as functions $U^*$ and $L^*$ at fixed values of $m^* = 5$ and $\zeta = 0.1$. It is observed that peak levels of $\eta$ reach a global maximum of 22.1% for $\left(L^*, U^*\right) = \left(0.5, 5.6\right)$.

Due to conservative estimation of the lift coefficient, the calculated efficiency is found to be less than the one of the original VIVACE [6,7] devive that is based on purely transverse vortex-induced oscillations of the cylinder, which can reach 33.2%. However, previous experimental assessment of the examined energy harvester yielded a maximum efficiency η of 31.4%; see [12].

In order to compare the oscillating foil energy converter to the hydrokinetic energy converter based on angular- induced vibrations in terms of energy conversion efficiency a suitable performance index should be devised. The oscillating foil sweeps a cross-section area equal to the area define by the maximum and minimum positions of the foil and the span of the device. The same principle is applied for the cylinder undergoing angular oscillations.

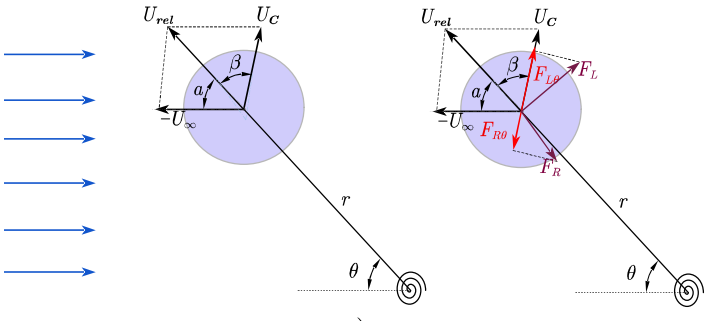


**Figure 5:** Two-dimensional model of the oscillating cylinder and vector diagram of the hydrodynamic forces acting on the cylinder.

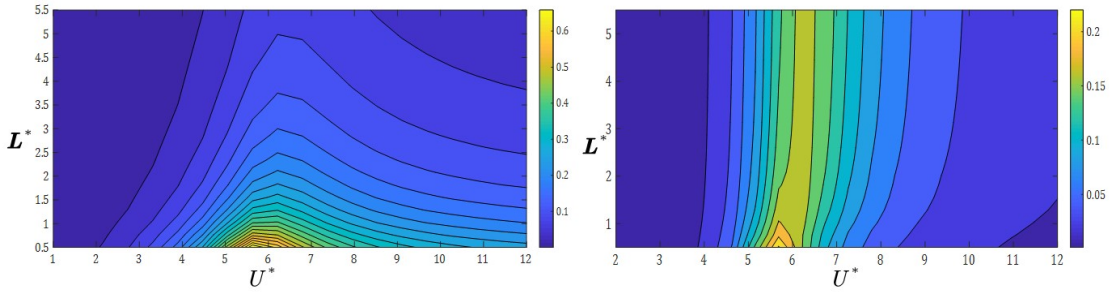


**Figure 6:** Response $A^*$ (left) and efficiency $\eta$ (right) of the oscillating cylinder device as functions of $L^*$ and $U^*$ for $m^* = 5$ and $\zeta = 0.1$.

Therefore, the power extracted by each device can be normalized by the power available for harnessing in the sweep area $S_{sw}$ , as follows

$$\eta = P_{net} / \left(0.5 \rho U^3 S_{sw}\right) . \tag{18}$$

Considering that the corresponding dimensionless quantity to the reduced velocity $U^*$ of VIV is the reduced frequency $k$ for the stream energy converter, the two devices operate at different range of frequencies. While the biomimetic converter operates for values around $k = 0.05 - 0.15$, the VIV device operates around a corresponding value $k = 0.2$. It is noticed that self – induced oscillating cylinder device operates in a very narrow bandwidth of frequencies, whereas the biomimetic stream energy converter is efficient for a wider range of frequencies. In VIV energy extraction, the elastic support must be designed in order to synchronize the natural frequency of the structure with the vortex shedding frequency, and since the VIV is a self-excited phenomenon, it cannot be prescribed. As a result, due to intense flow separation in the VIV case the "lock-in" phenomenon is a highly non – linear type of resonance, and it is quite difficult to achieve the synchronization between the vortex shedding and natural frequency of the structure. This is a fundamental difference compared to the biomimetic system, which has the advantage of setting the foil pitching motion, so that its performance is maximized. Thus, the biomimetic stream energy converter provides a more stable way of energy extraction from tidal currents, as it is shown to operate efficiently in a broader range of frequencies, at the cost of the requirement of an activation subsystem.

## 5 CONCLUSIONS

In this work, the performance of a biomimetic stream energy harvester, which includes a rotating, vertically mounted flapping wing, supported by an arm linked at a pivot point on its mid-chord section, is investigated through numerical modelling. The device is activated by an enforced self-pitching motion and the foil and the system perform angular oscillations around the vertical axis in parallel flow. For the unsteady analysis of the this flow energy harvester, a semi-3D model based on unsteady hydrofoil theory is developed and the obtained results are verified by comparisons with experimental data. Also, a linearized version of the model is derived in the frequency domain and is systematically applied in orderto study the effect of various parameters and reveal performance optimizations for the system. Finally, the biomimetic stream energy converter is compared against another type of flow energy extraction device, based on vortex – induced angular oscillation of a cylinder. It is shown that the latter system operates in a narrower bandwidth of frequencies, and since the VIV is a self – excited phenomenon, it is difficult to achieve synchronization between the shedding frequency (Strouhal frequency) and the natural frequency of the device. To conclude, the biomimetic stream energy converter operates in a wider range of frequencies thus offering the advantage of controlling the pitching amplitude.

## REFERENCES

[1] Xiao Q., Zhu Q. A review on flow energy harvesters based on flapping foils. *Journal of Fluids and Structures* (2014) **46**:174–191.

[2] Young J., Lai J., Platzer M.F. A review of progress and challenges in flapping foil power generation. *Progress in Aerospace Science* (2014) **67**:2-28

[3] Zhu Q., Haase M., and Chin H Wu. Modelling the capacity of a novel flow-energy harvester. *Applied Mathematical Modelling* (2009) **33**: 2207–2217

[4] Huxham G.H., Cochard S, and Patterson J. Experimental parametric investigation of an oscillating hydrofoil tidal stream energy converter. Proc. *18th Australasian Fluid Mechanics Conference (AFMC),* Launceston, Australia, 3-7 Dec. 2012.

[5] Kloos G, Gonzalez C.A., Finnigan T.D, The bioSTREAM tidal current energy converter, *Proceedings European Wave & Tidal Energy Conference*, EWTEC2009.

[6] Bernitsas, M.M., Raghavan, K., Ben-Simon, Y.Y., Garcia, E.M. VIVACE (Vortex Induced Vibration Aquatic Clean Energy: A New Concept in Generation of Clean and Renewable Energy From Fluid Flow. *ASME J. Off. Mech. Arct. Eng.* (2008) **130**, 041101.

[7] Lee, J., Bernitsas, M. High-damping, high-Reynolds VIV tests for energy harnessing using the VIVACE converter. *Ocean Eng.* (2011) **38**: 1697–1712

[8] Malefaki I., Belibassakis K. A model for performance estimation of flapping foil operating as biomimetic stream energy device. *J. Mar. Sci. Eng.* (2021) ***9***(1): 21.

[9] Malefaki I., Konstantinidis E., Assessment of a Hydrokinetic Energy Converter Based on Vortex Induced Angular Oscillations of a Cylinder, *Energies* (2020) **13**: 717

[10] Katz J., Plotkin A. *Low-speed aerodynamics*. Vol. 13, Cambridge Univ. Press (2001).

[11] Filippas, E., Belibassakis K.A. Hydrodynamic analysis of flapping-foil thrusters operating beneath the free surface and in waves. *Engineering Analysis with Boundary Elements* (2014) **41** 47-59.

[12] Arionfard, H., Nishi, Y. Experimental Investigation of a Drag Assisted Vortex-Induced Vibration Energy Converter*, Journal of Fluids and Structures* (2017) **68**: 48–57.